Coarsening, Modeling Grain Growth

Coarsening, or Ostwald ripening, occurs in a wide variety of two-phase mixtures ranging from liquid–vapor mixtures, such as raindrops in the atmosphere, to solid–solid mixtures, such as precipitates in a crystalline matrix. In each of these mixtures, the coarsening process can occur by the transport of some quantity, such as heat or mass, from regions of high interfacial curvature to regions of low interfacial curvature. This causes interfaces with low curvature to grow at the expense of interfaces with high curvature and the average size-scale of the domains to increase in size with time. The driving force for this process is the minimization of the total interfacial energy of the system. Coarsening typically occurs under conditions where the volume fractions of the phases are nearly at their equilibrium values. The coarsening process has a profound affect on the properties of materials. For example, in solid–solid mixtures the coarsening process can control the size of precipitates in solid–solid mixtures. This average particle size then sets the mechanical properties of the precipitation-hardened materials. In solid–liquid mixtures coarsening affects the average dendrite arm spacing and this spacing controls the degree of microsegregation in a casting.

The morphology of the second-phase domains that are undergoing coarsening can also be a strong function of the particular two-phase mixture. For example, the interfacial morphology of the solid dendrites in a liquid immediately following solidification, and two-phase mixtures following a spinodal decomposition process, display regions of both positive and negative curvature. In solid–solid mixtures the morphologies of precipitates can be cubes, plates, or even octagons, and thus can be highly anisotropic.

In an effort to focus on the physics governing the coarsening process, it is assumed that the system consists of a polydisperse array of spherical particles where the kinetics of the coarsening process are controlled by isothermal transport of the solute. This description is easily mapped to systems where coarsening proceeds by the transport of heat, such as in pure solid–liquid systems.

A qualitative understanding of the mechanism responsible for the ripening process can be understood by considering the composition field in the matrix between two spherical β-phase particles of different radii in an α matrix. Assuming local interfacial equilibrium the composition at the interface in the matrix is given by the Gibbs–Thompson equation:

$$C(R) = C_{\alpha}^{e} + l_c/R \tag{1}$$

where C is the mole fraction of component 1, C_{α}^{e} and C_{β}^{e} are the equilibrium compositions of α and β, respectively, as given by the phase diagram, and the capillary length l_c is given by:

$$l_c = \frac{2V_m\gamma}{(C_{\alpha}^{e} - C_{\beta}^{e})G_{\alpha}^{''}} \tag{2}$$

where V_m is the molar volume of α and β (assumed equal), γ is the interfacial energy, $G_{\alpha}^{''} = \delta^2 G_{\alpha}/\delta C^2$ evaluated at C_{α}^{e}, G_{α} is the molar free energy of α, and R is the radius of a particle. Thus, the particle with the smaller radius has a higher interfacial composition in the matrix than the larger particle. This, in turn, induces a concentration gradient in the matrix that causes solute to diffuse from the small particle to the large particle. This causes the small particle to shrink and the large particle to grow. The important insight provided by this picture is that the kinetics of the process are controlled by the diffusion of solute through the matrix subject to the interfacial concentrations as set by the Gibbs–Thompson equation.

1. Zero Volume Fraction

Consider the limit where there is no diffusional interaction between the particles. This implies that the distance between the particles is infinite, or, the volume fraction of particles is zero. This is clearly an oversimplification, but it captures much of the essential physics. This approximation was used by Lifshitz and Slyozov and Wagner (LSW) their classic work on coarsening (Lifshitz and Slyozov 1960, Wagner 1961). The description of the coarsening process to be developed below involves three equations that describe: (i) the growth rate of a particle of size R; (ii) the temporal evolution of a particle size distribution; and (iii) the global conservation of solute.

The system shall consist of a dispersion of spherical particles of β embedded in a matrix α. The molar volumes of β and α are taken to be identical. The interfacial energy between the α and β phases is isotropic. The two-phase mixture is assumed to be a binary alloy; extensions to ternary and higher order alloys have been made (see Kuehmann and Voorhees 1996 and references therein). The intrinsic diffusivities of each component are assumed to be equal and isotropic. We also assume that the interface is in local equilibrium.

The diffusion field surrounding a particle is given by a solution to the diffusion equation in the quasi-stationary approximation:

$$\nabla^2 C = 0 \tag{3}$$

Thus, the time derivative of the concentration field in the matrix is neglected. This is reasonable since the rate of change of the concentration field is much faster than the growth rate of a particle during coarsening.

The boundary conditions needed to solve Eqn. (3) are:

(i) the concentration in the matrix at the interface as given by the Gibbs–Thompson equation, Eqn.(1);

(ii) the concentration attains a value $C_\infty(t)$ at an infinite distance from a particle.

Boundary condition (ii) is consistent with our assumption that the distance between the particles is infinite. However, this matrix concentration must be time-dependent to satisfy mass conservation. The final condition necessary to determine the growth rate of a particle of radius R is the mass balance condition at the interface $r = R(t)$,

$$(C_\beta^e - C_\alpha^e)\frac{dR}{dt} = D\frac{\partial C}{\partial r} \tag{4}$$

where D is the interdiffusion coefficient, and t is time.

Solving Eqn. (3) subject to the boundary conditions yields the growth rate of a particle of a given size:

$$\frac{dR}{dt} = \frac{D}{R(C_\beta^e - C_\alpha^e)}\left(C_\infty(t) - C_\alpha^e - \frac{l_c}{R}\right) \tag{5}$$

Equation (5) implies that all particles larger than $C_\infty(t) - C_\alpha^e$ grow, and all particles smaller than $C_\infty(t) - C_\alpha^e$ shrink.

The particle size distribution evolves with time according to

$$\frac{\partial f(R,t)}{\partial t} + \frac{\partial (f(R,t)\,dR/dt)}{\partial R} = 0 \tag{6}$$

where $f(R, t)dR$ is the number of particles per unit volume of size R to $R + dR$. It is thus normalized such that

$$n_v = \int_0^\infty f(R,t)dR \tag{7}$$

where n_v is the total number of particles per unit volume in the system. Employing this equation assumes that particles of a given size are not created spontaneously (nucleated) and that particle coalescence does not occur.

The global mass conservation condition fixes the last unspecified variable in the problem, $C_\infty(t)$. Since the total amount of solute in the system is conserved and the concentration gradients during coarsening are typically,

$$C_0 = C_\infty + \phi(C_\beta^e - C_\alpha^e) \tag{8}$$

where C_0 is the alloy composition, ϕ is the volume fraction of coarsening phase, and we have assumed that $l_c/\langle R\rangle \ll 1$, where $\langle R\rangle$ is the average particle radius. Finally, the volume fraction of β is related to the particle size distribution by

$$\phi = \frac{4\pi}{3}\int_0^\infty R^3 f(R,t)dR \tag{9}$$

The analysis of Lifshitz and Slyozov and shows that in the limit of $t \to \infty$ the average particle size increases with time as $t^{1/3}$ and, furthermore, that the prefactor of this power law, beyond a collection of materials parameters, has a value of 8/9. Specifically,

$$\langle R\rangle^3(t) = K_{LSW}t \tag{10}$$

where K_{LSW} is the Lifshitz–Slyozov–Wagner rate constant

$$K_{LSW} = \left(\frac{8V\gamma D}{9(C_\beta^e - C_\alpha^e)^2 G_\alpha''}\right) \tag{11}$$

The supersaturation in the matrix decays as $t^{-1/3}$:

$$C_\infty(t) = C_\alpha^e\left(\frac{9(V\gamma)^2}{D(C_\beta^e - C_\alpha^e)(G_\alpha'')^2}\right)^{1/3} t^{-1/3} \tag{12}$$

The number of particles per unit volume decays as t^{-1}:

$$n_v(t) = 1.99\left(\frac{3(C_\beta^e - C_\alpha^e)^2 G_\alpha''}{8\pi V\gamma}\right) t^{-1} \tag{13}$$

where the factor 1.99 follows from a numerical evaluation of the moments of the time-independent distribution function.

Another result of asymptotic analysis is that when the particle size distribution $f(r, t)$ is scaled by the average particle size, *it should become time-independent*. This self-similarity implies that given sufficient time all particle size distributions, when scaled by $\langle R\rangle$, should assume a unique time-independent form, see Fig. 1. Figure 1 also shows that at zero volume fraction there is no particle in the system larger than $(3/2)\langle R\rangle$ and that the particle size distribution is skewed strongly towards the larger particle sizes.

2. *Nonzero Volume Fractions*

When the separation between particles is finite, it is necessary to account for interparticle diffusional interactions. The methods employed in these nonzero volume fraction theories have been reviewed (Voorhees 1984,Voorhees 1992). A qualitative understanding of the effects of a nonzero volume fraction of coarsening phase on the dynamics of the ripening problem can be obtained by considering the change in

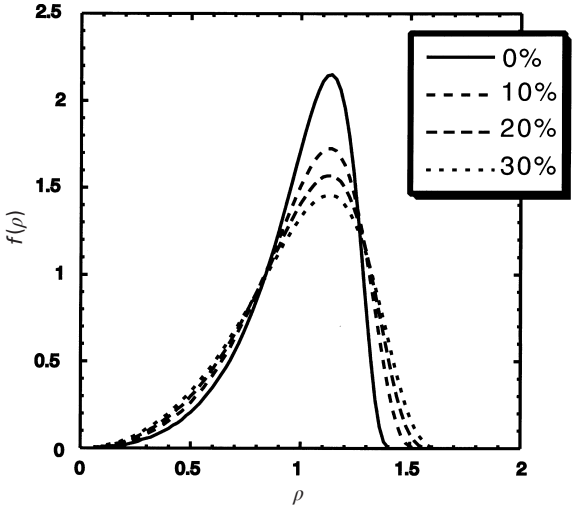

Figure 1
Particle size distributions as a function of $\rho = R/\langle R\rangle$, derived from the theory of Tokuyama *et al.* (Tokuyama *et al.* 1986) for various volume fractions. The LSW prediction is the 0% distribution.

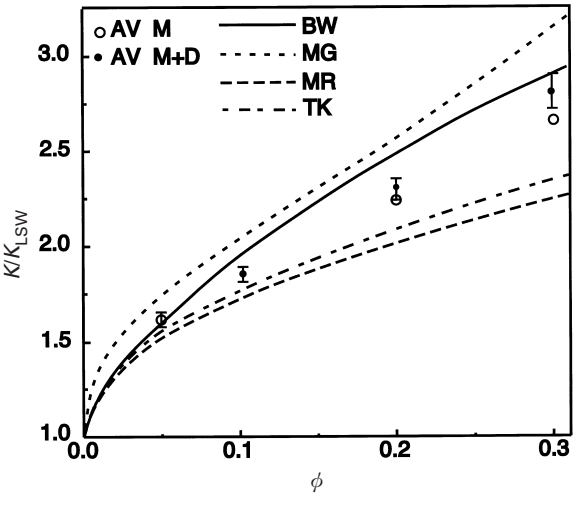

Figure 2
Rate constant as a function of the volume fraction due to the theories of AV (Akaiwa and Voorhees 1994), TK (Tokuyama *et al.* 1986), BW (Brailsford and Wynblatt 1979), MG (Marsh and Glicksman 1996), and MR (Marqusee and Ross 1984).

growth rate of two particles of different radius as they approach one another. Since the concentration in the matrix at the interfaces of each particle are different, as the distance between these two particles decreases the concentration gradients at the interfaces of each particle must increase. In fact, when the two particles touch the gradient between the two particles is infinite. Since the growth rate of a particle is directly proportional to the concentration gradient (see the mass balance equation Eqn. (4)) the growth rates of the particles increase as the interparticle separation decreases. Thus one would expect the coarsening rate of the system to increase as the volume fraction of particles increases.

However, what is not so obvious, but has been shown by many theories, is that a nonzero volume fraction does not alter the exponents of the temporal power laws but only affects the prefactors of the power laws. Thus, for example, the power law for the average particle radius becomes

$$\langle R\rangle^3(t) = K(\phi)t \tag{14}$$

where K is a monotonically increasing function of the volume fraction ϕ (Fig. 2). As seen in Fig. 2, there is a very rapid increase in the rate constant at small volume fraction, and by a volume fraction of 0.3 the rate constant is about a factor of 3 greater than that predicted by LSW. Most theories are not valid for volume fractions in excess of 0.3 as they assume that the particles are spherical. At volume fractions in excess of 0.3 it is necessary to employ the effective medium theories, such as those presented by Brailsford and Wynblatt (1979) and Marsh and Glicksman (1996).

Another phenomenon that is possible at nonzero volume fractions is the development of spatial correlations between the particles. In the zero volume fraction limit, the coarsening rate of a particle is a function only of its radius and the value of the concentration at infinity. Thus all particles of the same radius coarsen at the same rate. This will not be the case in a nonzero volume fraction system. If a particle of a given radius is surrounded by particles that are larger than itself it will tend to shrink, whereas if the particle is surrounded by particles that are smaller than itself it will tend to grow. This leads to particle spatial correlations. For example, the average interparticle separation for a system undergoing coarsening is larger than that for a random distribution, since the strong diffusional interactions that occur when a large and a small particle are located close to each other causes this small particle to disappear. At longer interparticle separation distances, however, large particles tend to be surrounded by the small particles that are feeding solute to these growing large particles (Akaiwa and Voorhees 1994).

These theories also find, in agreement with LSW, that the particle size distribution becomes time-independent when scaled by the average particle size. However, the shape of the scaled particle size distribution becomes a function of the volume fraction, as shown in Fig. 1. Although the predicted shapes of the particle size distribution at a given volume fraction differ from theory to theory, the qualitative dependence of the shape of the size distribution on volume

fraction is the same: as the volume fraction increases the particle size distributions become broader and more symmetric.

3. Elastic Stress

The ripening process is not always driven solely by a decrease in the interfacial energy. For example, elastic stress can be present in many crystalline solids and thus both the elastic and interfacial energies can drive the coarsening process. This elastic stress can result from many sources, both intrinsic such as that due to the difference in lattice parameter between the precipitate and matrix, and extrinsic such as an applied stress.

The underlying reason why elastic stress has such a large effect on the coarsening process in solids is that the total elastic energy of the system can easily be of the same order as the total interfacial energy. This can be shown by examining the magnitude of a dimensionless parameter L (Thompson *et al.* 1997). L is a measure of the relative importance of the elastic and interfacial energies during coarsening, where $L = \varepsilon^2 l C_{44}/\gamma$. ε is the particle–matrix misfit, l is a characteristic length of an individual particle or average particle size in a system with many particles, and C_{44} is an elastic constant of a crystal with cubic elastic anisotropy. The misfit is proportional to the difference in lattice parameters between the two phases. It is clear that L is the ratio of a characteristic elastic energy $\varepsilon^2 C_{44} l^3$ to a characteristic interfacial energy γl^2. In many systems, even those with small misfits, it is easy for particles to attain a size during coarsening where L is of order 1 or larger. Since the elastic and interfacial energies are then of the same magnitude, the coarsening process is driven by a decrease in both the elastic and interfacial energies in the system. As the states with minimum interfacial energy can be different from those with minimum elastic energy, fundamentally new coarsening dynamics can be expected.

The qualitatively different behavior of a system coarsening in the presence of elastic stress, compared with a system in the absence of stress, is illustrated by many theoretical and experimental investigations. Ardell and Nicholson (1996) showed clearly that with increasing size, or L, particles change their morphology from spheres to cuboids and then to plate-like shapes during coarsening. A strong alignment of particles along the elastically soft directions of the crystal is also noted with increasing L. Theoretical investigations have shown that elastic stress can give rise to large-scale particle migration through the matrix, inverse coarsening where small particles *grow* at the expense of large particles, and the possibility of changes in the temporal exponents that describe the coarsening process (for a review see Voorhees 1992). The effect of elastic stress on the coarsening process is an active area of research.

Bibliography

Akaiwa N, Voorhees P W 1994 Late-stage phase separation: dynamics, spatial correlations and structure functions. *Phys. Rev. E* **49**, 3860–80

Ardell A J, Nicholson R B 1966 On the modulated structure of aged Ni-Al alloys. *Acta Metall.* **14**, 1295–1309

Brailsford A D, Wynblatt P 1979 The dependence of Ostwald ripening kinetics on particle volume fraction. *Acta Metall.* **27**, 489–97

Kuehmann C J, Voorhees P W 1996 Ostwald ripening in ternary alloys. *Metall. Trans. A* **27**, 937–43

Lifshitz I M, Slyozov V V 1960 The kinetics of precipitation from supersaturated solutions. *J. Phys. Chem. Solids* **19**, 35–50

Marqusee JA, Ross J 1984 Theory of Ostwald ripening: competitive growth and its dependence on volume fraction*J. Chem. Phys.* **80**, 536–43

Marsh S P, Glicksman M E 1996 Kinetics of phase coarsening in dense systems. *Acta Mater.* **44**, 3761–71

Thompson M E, Su C H, Voorhees P W 1997 The equilibrium shape of a misfitting precipitate. *Acta Metall. Mater.* **42**, 2107–22

Tokuyama M, Kawasaki K, Enomoto Y 1986 Kinetic equations for Ostwald ripening. *Physica A* **134**, 323–38

Voorhees P W 1984 The theory of Ostwald ripening. *J. Stat. Phys.* **38**, 231–52

Voorhees P W 1992 Ostwald ripening of two phase mixtures *Annu. Rev. Mater. Sci.* **22**, 197–215

Wagner C 1961 Theorie der Alterung von Niederschlägen durch Umlösen. *Z. Elektrochemie* **65**, 581–91

P. W. Voorhees

Encyclopedia of Materials: Science and Technology
ISBN: 0-08-0431526
pp. 1255–1259